Estimating Landslide Volumes Using LS-rapid Model -The 2000 Stože Landslide in NW Slovenia

Jošt SODNIK[1,2*], Matej MAČEK[1] and Matjaž MIKOŠ[1]

[1] Faculty of Civil and Geodetic Engineering, University of Ljubljana (Jamova c. 2, 1000 Ljubljana, Slovenia)

[2] TEMPOS Environmental Civil Engineering Ltd. (Tehnološki park 21, 1000 Ljubljana, Slovenia)

*Corresponding author. E-mail: jost.sodnik@gmail.com

Potential landslides may after activation present a debris-flow source, and hence reliable potential landslide volume estimation is a significant factor when assessing regional debris-flow hazard. A 3D landslide simulation model LS-Rapid was applied to analyze the triggering phase of the rainfall-induced 2000 Stože Landslide in NW Slovenia, Europe. It was triggered on a steep Stože slope in November 2000. The destabilized mass moved and fluidized, and flowed as a dry debris flow to a torrent channel; due to inflow of rainfall and flow from the Mangartski potok torrent, after 35h it turned into a wet debris flow that reached the village of Log pod Mangartom, several kilometers away from the landslide source area. The known volume of the 2000 Stože Landslide was estimated using LS-Rapid simulation results. In addition, other parameters of the 2000 Stože Landslide (e.g. triggering factors, landslide source area, landslide contour, volume and depth, super elevation on its path, deposition area) were used to validate the LS-Rapid modeling results. Based on this case study, limiting boundaries for key soil parameters in the LS-Rapid model were proposed to help with the LS-Rapid model data preparation, when the model is applied for potential landslides where no model validation and calibration is possible, and when no ring-shear apparatus is at hand to estimate soil parameters.

Key words: debris flow, event magnitude, hazard assessment, landslide simulations

1. INTRODUCTION

Landslides and variety of their forms are focus of worldwide landslide research efforts for decades. An important part of the on-going research is how to assess landslide hazard, i.e. connecting their triggering (initation), transport (motion) and deposition (reach-out) phases. As a result, many landslide models have been developed worldwide; for a recent review on landslide models see *Yavari-Ramshe and Ataie-Ashtiani* [2016], p. 1335, **Table 3**).

One of the 3D landslide simulation models is the LS-Rapid model developed to assess the initiation and motion of landslides triggered by earthquakes, rainfalls or the combined effect. This model has been originally developed in 1988 by *Sassa* [1988] and improved upon in 2004 [*Sassa et al*., 2004]; it is based on the measured landslide mass dynamic properties determined by applying a ring-shear apparatus [*Sassa et al*., 2014a]. Its theoretical background is described in detail in *Sassa et al*. [2010].

The LS-Rapid model has found many applications all over the world:

a) for the earthquake-induced landslide cases such as the 2006 landslide in the Leyte Island, Philippines [*Sassa et al*., 2010], the 1792 Unzen-Mayuyama megaslide in Shimibara, Japan [*Sassa et al*., 2014a], the Daguangbao Landslide triggered by the 2008 Wenchuan Earthquake [*Tsuchiya et al*., 2013], hypothetical Senoumi submarine megaslide in the Suruga Bay, Japan [*Sassa et al*., 2012], the 2016 Kumamoto earthquake-induced Takanodai and Aso-ohashi landslides on Kyushu Island, Japan [*Dang et al*., 2016], the deep large-scale 2008 Arotazawa Landslide, Japan with a combined effects of seismic loading and pore pressure increase including volume increase during its motion [*Setiawan et al*., 2016; 2017] etc.;

b) for rainfall-induced landslide cases such as for the Kostanjek Landslide, Croatia [*Gradiški et al*., 2013], landslides at Iwa Valley area of Enugu State, Nigeria [*Igwe et al*., 2014], the 2009 Marappalam landslide in Tamil Nadu state, India [*Senthilkumar et al*., 2017], the 2015 rapid landslide at Ha Long City, Vietnam [*Loi et al*., 2017], the multi-stage Montaguto Earthflow, Italy [*Cuomo et al*., 2017], the formation of the

2011 Akatani Landslide dam in Kii Peninsula, Japan [*Tien et al*., 2017], the 2014 Hiroshima landslide disasters [*Sassa et al*., 2014b], the reactivated Grohovo Landslide, Croatia [*Arbanas et al*., 2017] and the Valići Landslide, Croatia [*Vivoda Prodan and Arbanas*, 2017] etc.;

c) for regional landslide susceptibility analyses such as for the Istrian Peninsula, Croatia [*Dugonjić Jovančević et al*., 2013; *Dugonjić Jovančević and Arbanas*, 2017], and the Koroška Bela landslides, Slovenia [*Sodnik et al*., 2017], as well as for the precursor stage of the Haivan Station Landslide, Vietnam [*Quang et al*., 2017].

The purpose of this study was to evaluate the 3D landslide simulation model LS-Rapid as a tool to estimate potential landslides volumes that once triggered can be debris-flow sources, and the estimated landslide volume can be used as the estimation of the maximum debris-flow magnitude. All this has a sense, if there is not enough field data available to perform a statistical (empirical) analysis of debris-flow magnitudes, as is the case in a small country such as Slovenia (20,273 km^2), where debris flow hazard is increasing in last two decades [*Mikoš and Majes*, 2012]. We used the well-investigated 2000 Stože Landslide case study as the validation case for the model LS-Rapid, with a goal to be able to use it in future for regional landslide susceptibility analyses, as well as for estimation of maximum debris-flow magnitudes triggered on slopes as landslides.

2. THE 2000 STOŽE LANDSLIDE

The Stože Landslide was triggered after intensive rainfall in November 2000 [*Mikoš et al*., 2004] (for location see **Fig. 1**).

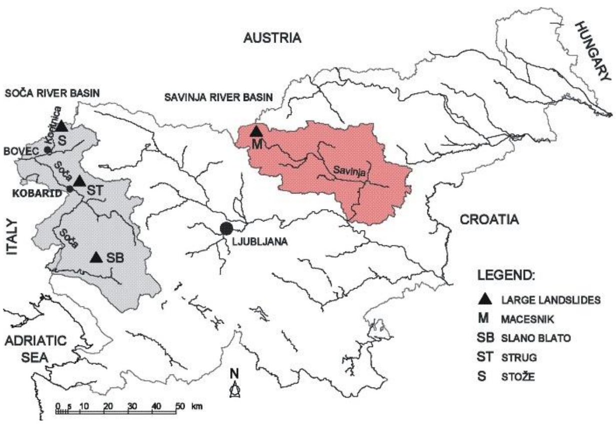

Fig. 1 The 2000 Stože Landslide and other recent large landslides in Slovenia (volume > 1 mio m^3) [*Mikoš et al*., 2004].

On November 15, 2000 in the first phase, landslide was triggered and stopped in the Mangartski potok torrent. The landslide was triggered on the altitude between 1200m and 1600m a.s.l. In the second phase on November 17, 2000, after additional 36h of rain and inflow of the Mangartski potok discharge, the deposited landslide mass turned into a wet debris flow and destroyed part of the village Log pod Mangartom and caused 7 casualties [*Mikoš*, 2011]. This was one of the most devastating landslides in the last century in Slovenia [*Mikoš and Majes*, 2012].

The second phase of the wet debris flow was investigated by applying debris-flow numerical modelling in order to assess debris-flow hazard in the area under assumption that potential debris flows can be triggered on the Stože slope [*Četina et al*., 2006].

The triggering phase was not investigated in details and results of such a study with a landslide triggering simulation would be useful for investigating potential landslides as debris flow sources. In this study, the LS-Rapid model was used to simulate triggering of the Stože landslide (the first phase of the 2000 event), and to compare simulation results with the field observations during the two-stage event and the post-event field investigations.

On November 15th 2000, the Stože landslide was triggered as a relatively dry debris slide (1st phase), and then, on November 17th 2000, turned into a wet debris flow (2nd phase). The main cause of the Stože landslide was prolonged heavy rainfall. The measured rainfall at Log pod Mangartom village was 1638 mm in the previous 48 days, which presents a recurrence interval of more than 100 years. In the first phase, a "dry" slide was triggered on the slope and the landslide mass stopped in the Mangartski potok torrent channel with a slope of 16%. During the next 36 h, the landslide mass was additionally wetted by heavy rainfall and a direct water inflow from the Mangartski potok. Early on 17 November 2000, a second event happened. The previously deposited landslide mass turned into a wet debris flow that travelled for approximately 5 km with approx. 500 height difference. In the village of Log pod Mangartom, the debris flow on its way destroyed 6 houses and severely damaged 23 houses, and caused 7 casualties. The simulated debris-flow velocities in the steepest part of the Mangartski potok channel of 45° were up to 60 km/h. [*Četina et al.*, 2006].

3. LS-RAPID SIMULATION MODEL

For the topographic data of the Stože debris-flow numerical model a new LiDAR-based DTM with the resolution of 1 m was used. At the location of the landslide, the DTM was manually using CAD tools corrected to the original state before the 2000 event based on topographic maps in scale 1:5000. With a combination of both data in CAD tools, a pre-event topography of the triggering area was made to be used in the simulation model (**Fig. 2**). For the determination of geological units and soil parameters for the LS-Rapid model, the Basic Geological map of Slovenia in scale 1:100,000 was used (**Fig. 3**).

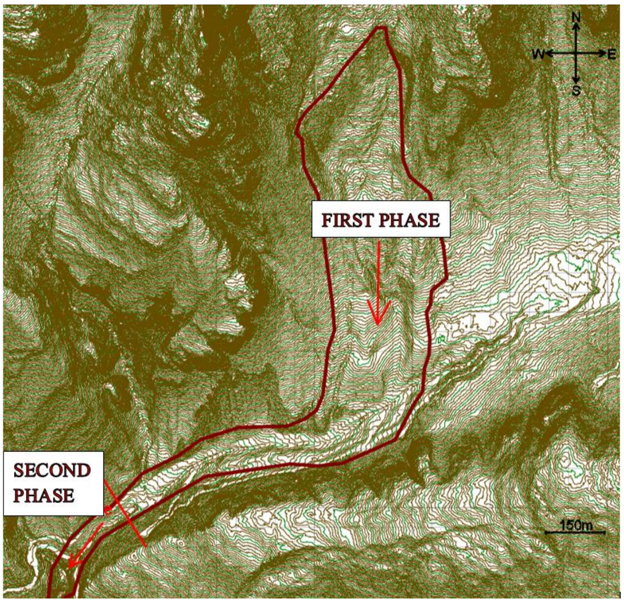

Fig. 2 Pre-event topography of the case study area with the contour of the Stože landslide.

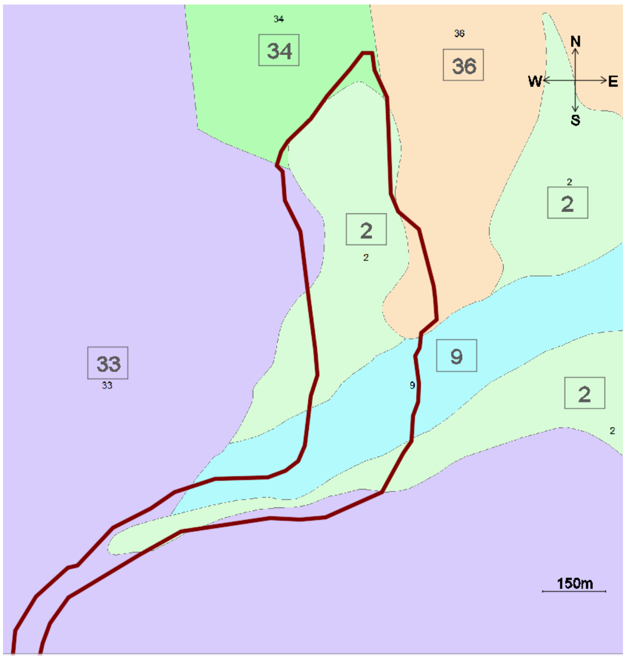

Fig. 3 Geological map of the area: 33 – bedded dolomite; 34 – limestone, marlstone, dolomite; 36 – massive or bedded dolomite; 2 – Scree; 9 – moraine**.**

Soil parameters and the depth of unstable mass for each geological unit on the Stože slope were assessed based on the geotechnical laboratory test results, expert experience and judgement.

With additional topographical analysis, we determined geological units where terrain slope exceeds the angle of internal friction of the soil. In reality, these areas are steep bare weathered rocks with no or sporadic soil cover and are more prone to rock falling then sliding.

After this analysis, the two "potentially unstable" geological units were "scree material" and "moraine". For these two units soil parameters were assessed, and detail conditions are described in chapter 5. To determine τ_{ss} (steady state shear resistance at the sliding surface) authors of the model suggested to use an undrained ring-shear apparatus of this type, such as ICL-1 to ICL-3 [e.g. *Oštrić et al.*, 2012].

No tests were performed in a ring shear apparatus, since it was not available at the time of the laboratory testing and has limitations in terms of the maximum grains size of the mixture (2mm). More than 60% of the landslide mass has grain sizes over 2mm that makes ring-shear apparatus less useful when modelling landslides in the European Alpine environment. [*Maček et al.*, 2017].

Due to these limitations, a following relationship was proposed Eq. (1) between τ_{ss} and τ_p (peak/maximum shear resistance before failure).

$$\tau_{SS} \approx 0.45\tau_p \xrightarrow{up\ to} 0.65\tau_p \tag{1}$$

Other soil parameters were proposed based on experiences with laboratory testing and professional judgement: Scree material: K_0=0.5; ϕ_i=40°; ϕ_m=40°; τ_{ss}=190kPa; B_{ss}=1.0; ϕ_p=42°; c_p=5.0kPa; γ=22KN/m^3; and Moraine: K_0=0.5; ϕ_i=36°; ϕ_m=36°; τ_{ss}=190kPa; B_{ss}=1.0; ϕ_p=37°; c_p=25kPa; γ=23KN/m^3, where K_0 is lateral pressure ratio, ϕ_i friction coefficient inside landslide mass, ϕ_m friction coefficient during motion at sliding surface, τ_{ss} steady state shear resistance at sliding surface, B_{ss} rate of excess pore-pressure generation, ϕ_p peak friction coefficient at sliding surface, c_p peak cohesion at sliding surface, and γ unit weight of mass).

Based on the available borehole data, a soil depth (potentially unstable mass) of 30m was used in the model for both geological units. For better presentation of the real conditions, a "smoothing" function was applied to ensure smooth increase at the landslide edges from 0 to 30m in the middle of the debris slide area.

The LS-Rapid model includes two triggering factors: earthquakes and pore pressure. In case of the Stože landslide, the increase of pore pressures triggered the landslide. The LS-Rapid model uses pore pressure ratio (r_u) for determination of pore pressures in the landslide body.

$$r_u = \frac{h_w \gamma_w}{h_m \gamma_m} \qquad (2)$$

Therefore, r_u=0.3, based on Eq. (2) presents approx. water table at 67%-layer height and r_u=0.45 represents water table at ground surface. In our simulations, r_u=0.3 was used, as one of possible realistic scenarios. On the other hand, r_u=0.45 represents full saturation and so called "worst case scenario".

4. SIMULATIONS OF THE 2000 STOŽE LANDSLIDE

4.1 Triggering simulation

Fig. 4 shows model topography with unstable mass (scree and moraine). Other parameters of the model were set as: simulation time of 100 s with time step 0.005s, shear displacement at the point of failure *DL*=1 mm, and at the end of shear strength reduction *DU*=1000 mm.

The simulation purpose was to analyse the triggering phase of the Stože landslide and to compare the modelling results with the surveyed landslide contour, traveling distance of the first phase e.g. "dry" slide and the landslide volume.

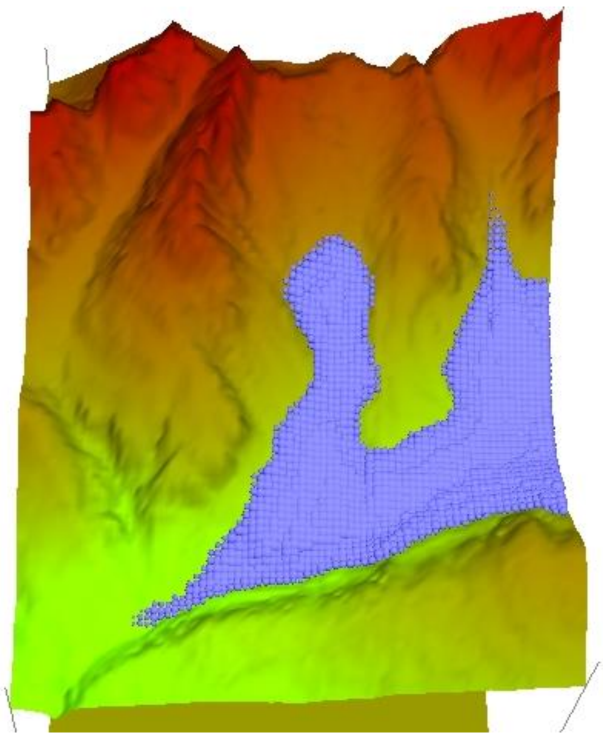

Fig. 4 Model topography and unstable mass.

Table 1 LS-RAPID model topography and results legend

Color	Moving mass thickness (m)
(blue)	stable mass
(yellow)	0-6
(orange)	6-12
(light red)	12-18
(red)	18-24
(dark red)	24-30
(darkest red)	>30

In **Table 1** colors of the simulation topography and modeling results are shown. Different colors represent the thickness of the moving mass.

Unstable and moving mass is presented as balls, which is one of the options in the model. Larger radius of the ball means thicker unstable or moving mass. Size of the largest ball is defined with maximum thickness of the unstable mass at the start of the simulation. During simulation size of the balls does not change, therefore this kind of modelling presentation is more suitable for graphical presentation. For exact measurements and calculations of the moving mass thickness, one has to use txt (matrix) output files where exact thickness is given for each simulation step of the modelling process.

4.2 Sensitivity analysis of the model

A sensitivity analysis of τ_{ss} and r_u parameters was carried out to determine the influence of each parameter on the simulation results and to determine the soil parameters of the model that is closest to real landslide behaviour.

4.2.1. Influence of r_u

For analysis of influence of pore pressure ratio, we chose fixed value τ_{ss}=150kPa and changed values of r_u in the following steps: r_u=0.0 (no pore pressure); r_u=0.1; 0.2; 0.3; 0.4 and 0.45 (ground water table at slope surface).

For r_u value estimations we used relationship proposed with Eq. (2). We used different values of r_u and compared the simulation results in the initial and final state of simulation. On **Fig. 5** we can see that with no pore pressure there is no unstable areas and no landslides are triggered. But on **Fig. 6** we can see that with high pore pressure ratio numerous areas become unstable, even outside of the surveyed 2000 Stože Landslide contour. This result shows that higher pore pressures could lead to even larger magnitudes of the 2000 event. With enlarging r_u values more unstable areas are simulated, therefore the movement of the landslides depends more on the τ_{ss} value which will be presented in the following chapter.

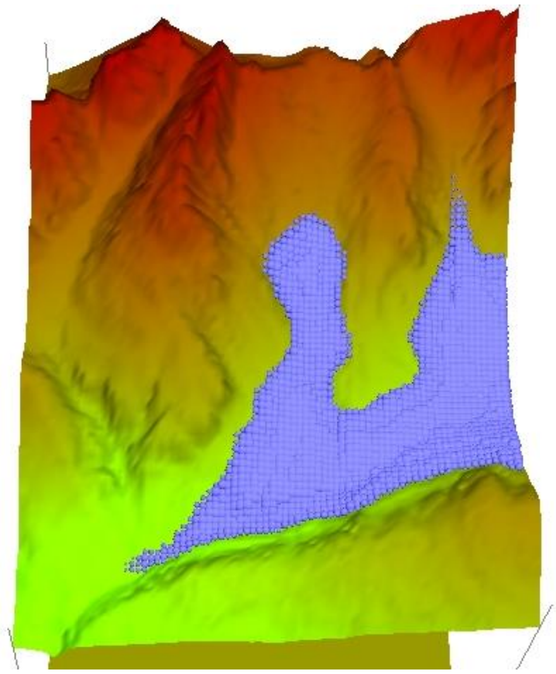

Fig. 5 Final simulation result with r_u=0.0.

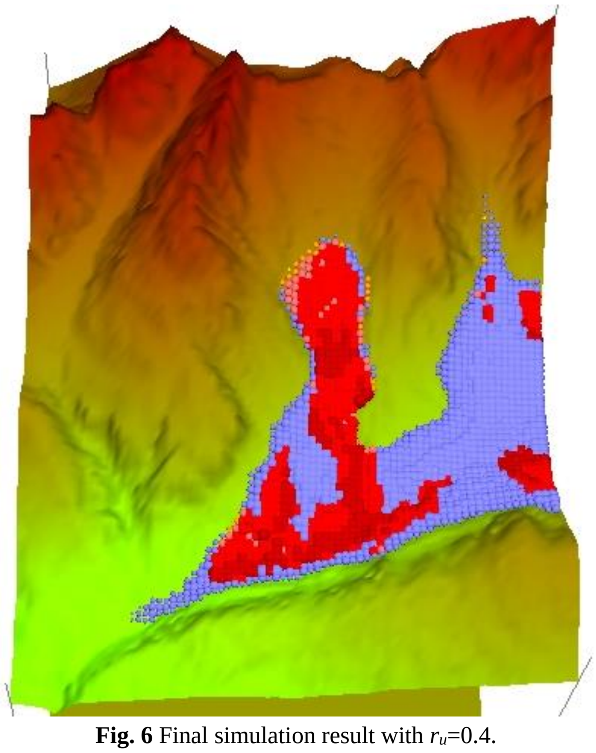

Fig. 6 Final simulation result with r_u=0.4.

On **Fig. 7** we can see that value r_u=0.2 causes unstable areas inside Stože landslide area, but in much smaller amount then surveyed on the field (**Fig. 2)**. These results show that r_u value defines unstable areas in the model, but the spreading of unstable areas and landslide movement depend on τ_{ss} value. Also based on these results we concluded that r_u value of Stože landslide event was approx. 0.3.

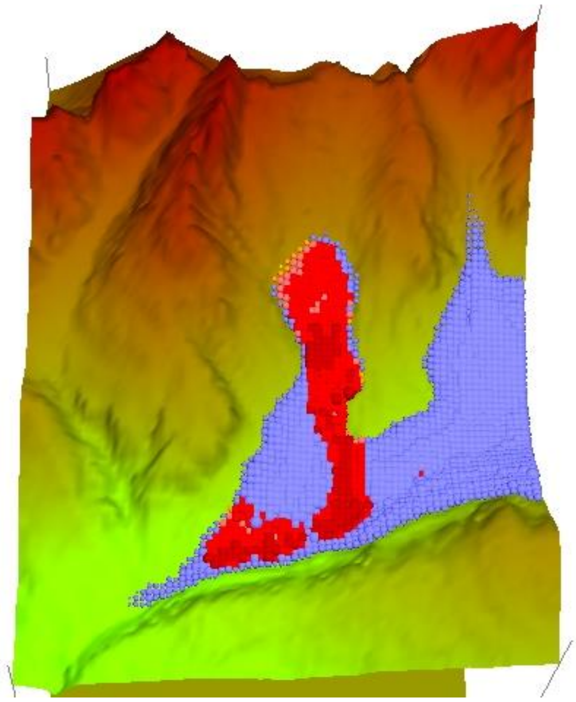

Fig. 7 Final simulation result with r_u=0.2.

4.2.2. Influence of τ_{ss}

After testing the influence of r_u parameter and conclusions about approx. value of November 2000 Stože landslide event, we tested influence of τ_{ss} parameter. We choose r_u=0.3 for all the models and changed τ_{ss} values with following steps: τ_{ss}=2 kPa (measured value after *Lenart and Fifer Bizjak*, 2010); 50 kPa (lower boundary after *Sassa et al*., 2010); 100 kPa; 150 kPa; 200 kPa, and 250 kPa. Models with low τ_{ss} values (**Fig. 8**) show that already in the initial phase all unstable areas start to spread and move. On the other hand, we can see (**Fig. 9**) that higher values of τ_{ss} prevent all the simulated area to collapse and move. Small spots of unstable areas can be found, but no spreading of instability or mass movement is simulated.

With low τ_{ss} values model simulates also very unrealistic scenarios. With τ_{ss}=2kPa after 10s practically all the modelling area is mobilized (**Fig. 10**), or even more unrealistic scenario with landslide mass splashing over the reef (**Fig. 11**) (approx. 200m height difference between Mangartski potok channel and reef height). In the calculation no viscosity effect on shear strength or non-frictional dissipation of energy was used. In case it would be used the spreading should be smaller. These results show realistic and correct values of τ_{ss} parameter are crucial for getting realistic and reliable simulation results.

With such differences in the simulation results, depending of τ_{ss} values, some first estimations before the simulation are necessary. Therefore, our proposal for τ_{ss} estimation in Eq. (1).

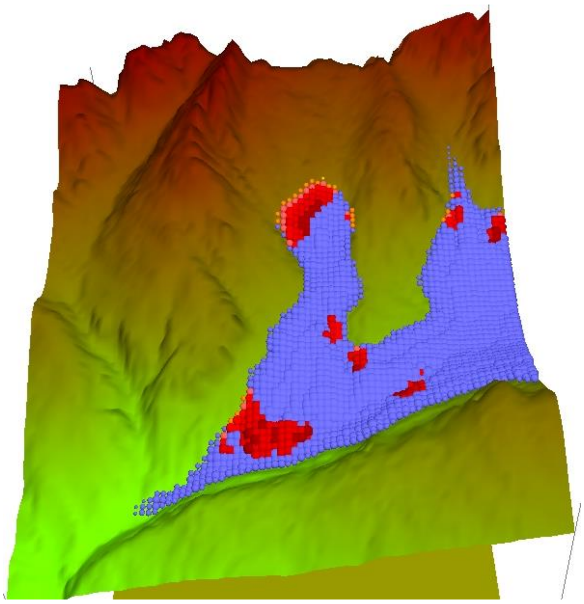

Fig. 8 Simulation result after 1s with τ_{ss}=2kPa.

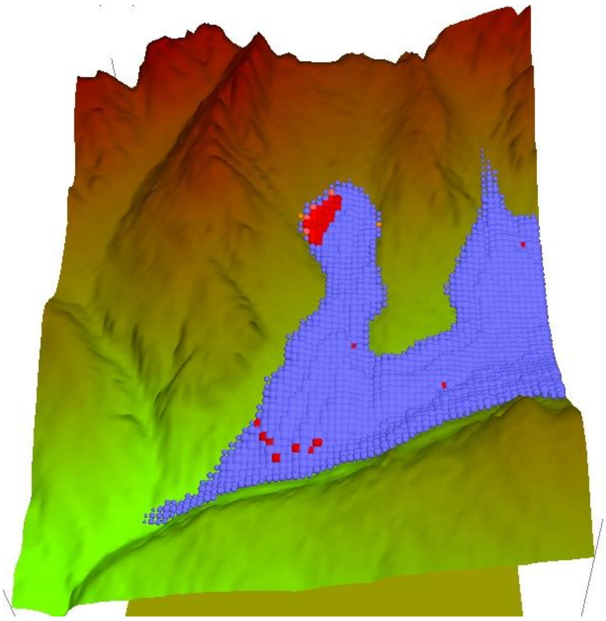

Fig. 9 Final **s**imulation result with τ_{ss}=250kPa.

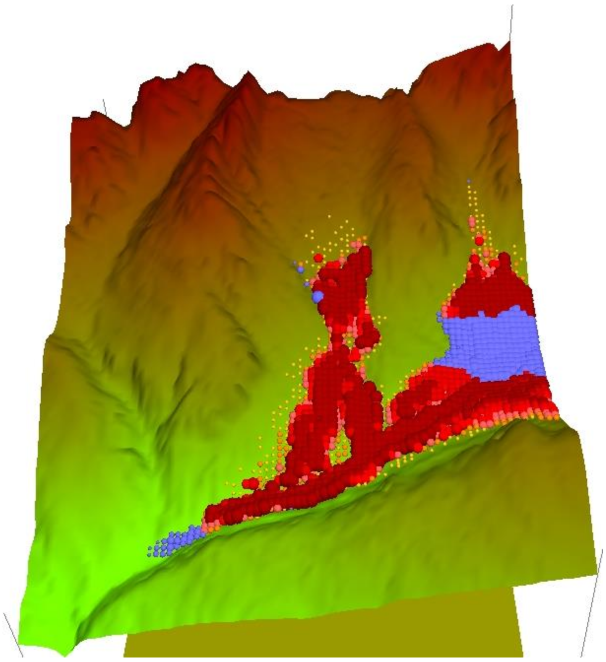

Fig. 10 Simulation after 10s at τ_{ss}=2kPa.

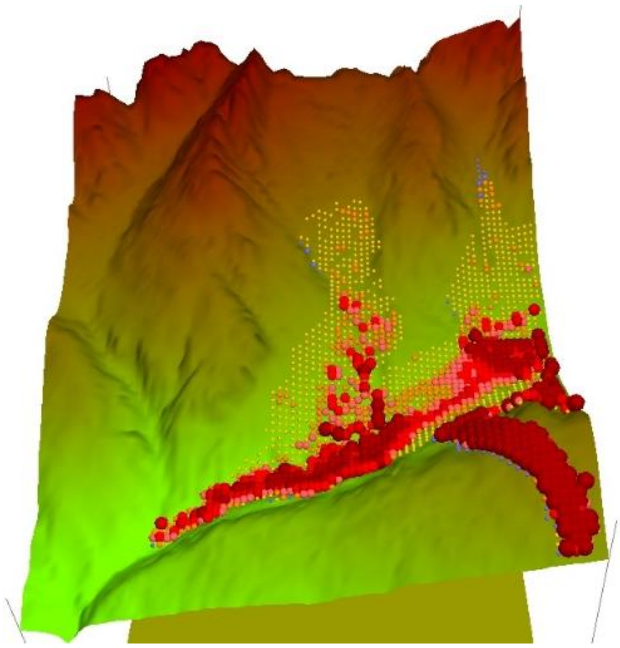

Fig. 11 Simulation after 27s at τ_{ss}=50kPa.

5. RESULTS

5.1 Contour of the 2000 Stože landslide

The comparison of the final simulated landslide area and the surveyed landslide contour after the 2000 event is presented in **Fig. 12**. A good agreement of the results and the surveyed contour is achieved.

In the upper part of the Stože landslide, the simulated area is narrower than the real contour, most likely due to inaccuracy of the basic geological map and therefore lower accuracy of the position and surface of each geological unit in the model. In the lower part of the Stože landslide, the simulated area is wider than the observed contour. The reason for this difference can be found in differences of the geological situation between the model and field situation or also in the fact that some of the areas are very prone to sliding, but in the November 2000 event, they did not move. Some unstable areas outside of the landslide (the upper right part in **Fig. 12**) could be found, but can also be related to the fact that this small unstable area lies at the model border where simulation conditions are not fully regular.

5.2 Traveling distance of the Stože landslide

In the phase 1 the Stože debris slide travelled to the small bridge over the Mangartski potok (Mlinč).

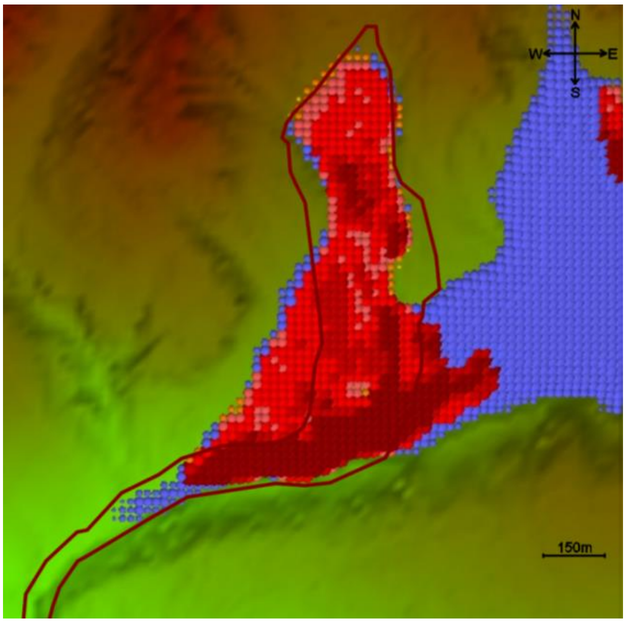

Fig. 12 LS-Rapid model results compared with surveyed landslide contour.

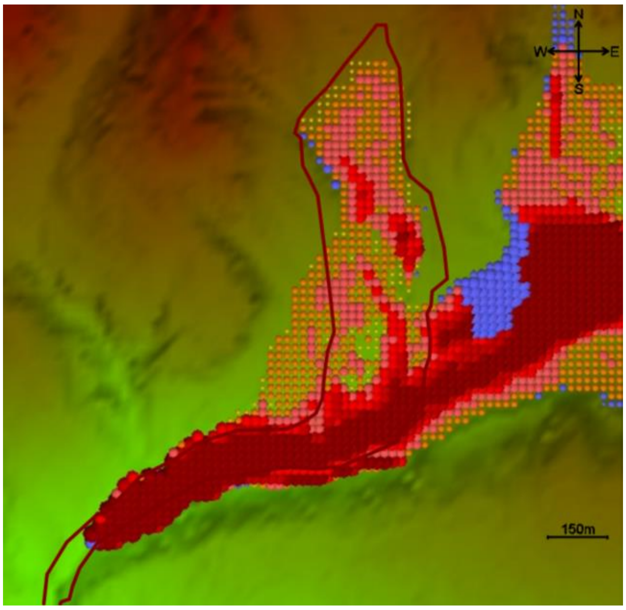

Fig. 13 Model with the correct traveling distance of the Stože landslide.

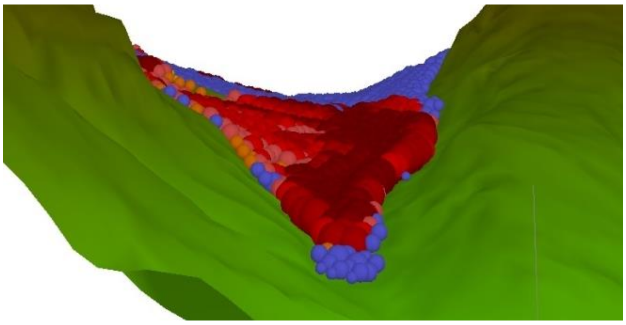
Fig. 14 Mangartski potok left bank final simulation conditions.

The final model results (**Fig. 12**) show stopping of the landslide mass upstream of the bridge, but the model with lower τ_{ss}=125kPa shows good agreement from that point of view (**Fig. 13**). The model with τ_{ss}=125kPa is however unsatisfactory in other comparisons (area, volume). It is possible that lower τ_{ss} values that are needed to stop the debris slide at the bridge and not upstream as in the modelling result, are caused by additional water inflow from the Mangartski potok, which lowers the τ_{ss} values on the field and cannot be modelled in one simulation.

Another specific characteristic of the first phase of the 2000 Stože Landslide were the conditions on the left bank of the Mangartski potok where the landslide travelled across the Mangartski potok channel and damaged the local road to the Mangart Mountain. **Fig. 14** shows the final simulation conditions/result on the Mangartski potok left bank where the flow super elevation is clearly seen. Red balls represent thickness of the material. Dark red is the thickest area and light red is the thinnest. Exact thickness of the material can be found in the matrix output data of the model. Blue color represents potentially unstable mass which did not move during simulation. Computational grid was selected at 20m x 20m.

5.3 The Stože landslide volume

A reliable estimation of the landslide volume is very important in the process of debris-flow hazard assessment since the landslide mass presents an important sediment source for the following debris flows. In the process of volume estimation, values of τ_{ss} and r_u were varied and the landslide volume for each combination was calculated (**Table 2**). All other parameters of the model remained the same as given in chapter 3.

Table 2 τ_{ss} and r_u combinations with landslide volume calculations.

τ_{ss} (kPa)	r_u	Volume (m^3)
150	0.2	2,480,00
200	0.2	735,000
250	0.2	51,000
150	0.3	2,460,000
180	0.3	1,547,000
190	0.3	1,195,000
195	0.3	990,000
200	0.3	775,000
250	0.3	72,000
200	0.35	800,000
150	0.4	2,470,000
200	0.4	825,00
250	0.4	105,000

The landslide volume was calculated using matrices of the input topography and the final simulated topography, respectively. The estimated volumes of the Stože landslide after the event were according to *Rajar et al*. [2001]: mobilized volume: 1,580,000m^3; material deficit volume: 1,200,000m^3; material stopped inside debris slide triggering area: 380,000m^3, and according to *Četina et al*. [2006]: 1,200,000m^3.

A comparison of the estimated volumes and the simulation results show that the best agreement is found with τ_{ss}=190kPa and r_u=0.3 with the simulated volume of 1,195,000m^3. With τ_{ss}=190kPa we confirmed our proposed τ_{ss}=0.45 x τ_p and τ_{ss}=0.45 x 421kPa=189kPa (Eq. (1)). The best agreement with the real landslide volume is obtained with the lowest boundary of τ_{ss} proposed by Eq. (1), while the upper limit gives unrealistically low landslide volumes.

6. THE SIMULATION AND MODEL ISSUES

First issue about the LS-Rapid model is matrix-based system with the matrix-based "user unfriendly" data input. That problem becomes important with geologically heterogeneous areas where each geological unit has different parameters and the manual data input becomes very time consuming and inaccurate. To solve this problem, we developed a MS Excel based application for the data matrix preparation. Additional functions were implemented in the matrix preparation as previously mentioned "smoothing" function for ensuring linear transition between two soil materials with a different depth of the unstable mass.

Second important issue of the model is that only one pore pressure ratio value as the triggering factor can be used for the whole area in the model. Again, with geologically heterogeneous areas this becomes an important issue since according to Eq. (2) not all units have the same specific weight (for instance scree and fine grain material) and therefore r_u factor is not comparable. To overcome this model issue, we propose that the angle of internal friction of the fine-grained geological units should be reduced in a model as given in Eq. (3).

$$\tan\varphi_{model} H\gamma\left(1-r_{u,model}\right) \approx \tan\varphi\, H\gamma\left(1-r_u\right) \tag{3}$$

where: φ is friction angle, φ_{model} is the angle of internal friction used in the model, γ is the unit weight of landslide mass, H is the depth of slip surface, r_u is the pore pressure ratio, and $r_{u,model}$ is the pore pressure ratio used in the model.

The determination of τ_{ss} should be carried out using LS-Rapid linked ICL-1 to ICL-3 ring shear apparatus. The maximum grain-size limitation of this apparatus (D_{max}=2mm) is an important issue when modelling landslides in the Alpine areas with prevailing gravel materials. This limitations of determining exact material parameters will bring some uncertainty in the performed calculations, especially when modelling potential events where model validation is not possible.

7. DISCUSSION

Debris flows present serious hazard in Alpine regions, including Slovenia, and debris-flow hazard assessment should be well implemented in the process of spatial planning and land use management. Since landslides often present a debris-flow source and the landslide volume is the main factor for debris-flow magnitude estimation, landslide-triggering simulation presents an important part in the process of debris-flow hazard assessment. Due to complexity of the landslide triggering phenomena this research topic is challenging with a goal of developing reliable methodology for potential landslide volume estimations. The results of our study present that a good estimation of key parameters and input data can result with good agreement of simulation results and field observations. LS-Rapid model has been recognized as a useful tool for landslide triggering simulations. However, the large differences in the modelled and observed landslide volumes were observed for different soil parameters. With this knowledge and experience, such an approach could be also used for potential landslide simulation and potential debris-flow magnitude estimation, taking into account possible range of volumes.

Besides soil parameters of the potential landslide, soil cover depth (depth of potentially unstable mass) is very important when simulating landslide triggering. This data should be available in the updated geological maps, which should be prepared in smaller scale (e.g. 1:10,000/1:25,000). Other more expensive option is to carry out detailed geological mapping of each potential debris-flow hazard area.

On the other hand, the proposed approach to landslide-triggering simulation, where only pore pressure is considered as the triggering factor, we see an opportunity for further model development and a link of the triggering model with a hydrological model. In this case, triggering pore pressures could be linked with hydrological process of precipitation, infiltration, direct runoff, and evapotranspiration and in the final phase determination of critical precipitation or precipitation triggering threshold.

ACKNOWLEDGMENT: The authors acknowledge the financial support from the Slovenian Research Agency (research core funding No. P2-0180).

REFERENCES

Arbanas, Ž., Mihalić Arbanas, S., Vivoda Prodan, M., Peranić, J., Sečanj, M., Bernat Gazibara, S., and Krkač, M. (2017): Preliminary Investigations and Numerical Simulations of a Landslide Reactivation, In: Mikoš, M., Tiwari, B., Yin, Y., Sassa, K. (eds.): Advancing Culture of Living with Landslides, Vol. 2 - Advances in Landslide Science, pp. 649-657.

Cuomo, S., De Chiara, V., Dugonjić Jovančević, S., Vivoda Prodan, M. and Arbanas, Ž. (2017): Insights from LS-Rapid Modeling of Montaguto Earthflow (Italy). In: Mikoš, M., Tiwari, B., Yin, Y., Sassa, K. (eds.): Advancing Culture of Living with Landslides, Vol. 2 - Advances in Landslide Science, pp. 611-619.

Četina, M., Rajar, R., Hojnik, T., Zakrajšek, M., Krzyk, M. and Mikoš, M. (2006): Case Study: Numerical Simulations of Debris Flow below Stože, Slovenia, Journal of Hydraulic Engineering, Vol. 132, No. 2, pp. 121-130.

Dang, K., Sassa, K., Fukuoka, H., Sakai, N., Sato, Y., Takara, T., Quang, L.H., Loi, D.H., Tien, P.V. and Ha, N.D. (2016): Mechanism of two rapid and long-runout landslides in the 16 April 2016 Kumamoto earthquake using a ring-shear apparatus and computer simulation (LS-RAPID), Landslides, Vol. 13, No. 6, pp. 1525-1534.

Dugonjić Jovančević, S., Nagai, O., Sassa, K. and Arbanas, Ž. (2013): Deterministic Landslide Susceptibility Analyses Using LS-Rapid Software. Proceedings of the 1st Regional Symposium on Landslides in the Adriatic-Balkan Region, Zagreb, pp. 73-77.

Dugonjić Jovančević, S. and Arbanas, Ž. (2017): Influence of the runout potential on landslide-susceptible areas along the flysch–karst contact in Istria, Croatia, Natural Hazards, Vol. 85, No. 3, pp. 1347-1362.

Gradiški, K., Sassa, K., He, B., Arbanas, Ž., Mihalič Arbanas, S., Krkač, M., Kvasnička, P. and Oštrič, M. (2013): Application of Integrated Landslide Simulation Model LS-Rapid to the Kostanjek Landslide, Zagreb, Croatia. Proceedings of the 1st Regional Symposium on Landslides in the Adriatic-Balkan Region, Zagreb.

Igwe, O., Mode, W., Nnebedum, O., Okonkwo, I. and Oha, I (2014): The analysis of rainfall-induced slope failures at Iva Valley area in Enugu State, Nigeria, Environmental Earth Sciences, Vol. 71, pp. 2465-2480.

Lenart, S. and Fifer Bizjak, K. (2010): Particularities of Stože and Lokavec landslides – special laboratory tests for landslides modeling, WSEAS Transactions on Environment and Development, Vol. 7, No. 5, pp. 355-364.

Loi, D.H., Quang, L.H., Sassa, K., Takara, K., Dang, K., Thanh, N.K. and Tien, P.V. (2017): The 28 July 2015 rapid landslide at Ha Long City, Quang Ninh, Vietnam, Landslides, Vol. 14, No. 3, pp. 1207-1215.

Maček, M., Smolar, J. and Petkovšek, A. (2017): Influences of rheometer size and the grain size on rheological parameters of debris flow. In: Mikoš, M., Tiwari, B., Yin, Y., Sassa, K. (eds.): Advancing Culture of Living with Landslides, Vol. 2 - Advances in Landslide Science, pp. 399-406.

Mikoš, M. (2011): Public Perception and Stakeholder Involvement in the Crisis Management of Sediment-Related Disasters and their Mitigation: the Case of the Stože Debris Flow in NW Slovenia, Integrated Environmental Assessment and Management, Vol. 7, No. 2, pp. 216-227.

Mikoš, M., Četina, M. and Brilly, M. (2004): Hydrologic conditions responsible for triggering the Stože landslide, Slovenia, Engineering geology, Vol. 73, No. 3/4, pp. 193-213.

Mikoš, M. and Majes, B. (2010): Mitigation of large landslides and debris flows in Slovenia, Europe, In: Landslides: Causes, Types and Effects, Nova Science Publishers, New York, pp. 105-131.

Oštrić, M., Ljutić, K., Krkač, M., Setiawan, H., He, B. and Sassa, K. (2012): Undrained ring shear tests performed on samples from Kostanjek and Grohovo landslide. In: Sassa, K., Takara, K. and He B. (eds.) Proceedings of the 10th Anniversary of ICL, January 2012, Kyoto, Japan, pp. 47–52.

Quang, L.H., Loi, D.H., Sassa, K., Takara, K., Ochiai, H., Dang, K., Abe, S., Asano, S. and Ha, D.N. (2017): Susceptibility assessment of the precursor stage of a landslide threatening Haivan Railway Station, Vietnam, Landslides, https://doi.org/10.1007/s10346-017-0870-3.

Rajar, R., Hojnik, T., Četina, M., Zakrajšek, M. and Krzyk, M. (2001): A one-dimensional model of a debris flow in the area of Log pod Mangartom, Proceedings 12. Mišičev vodarski dan, pp. 92-101 (in Slovene).

Sassa, K. (1988): Geotechnical model for the motion of landslides, Proceedings 5th International symposium on Landslides, “Landslides”, Vol. 1, Balkema, Rotterdam, pp. 37-56.

Sassa, K., Wang, G., Fukuoka, H., Wang, F., Ochiai, T, Sugiyama, M and Seguchi, T (2004): Landslide risk evaluation and hazard zoning for rapid and long-travel landslides in urban development areas, Landslides, Vol. 1, No. 3, pp. 221-235.

Sassa, K., Nagai, O., Solidum, R., Yamazaki, Y. and Ohta, H. (2010): An integrated model simulating the initiation and motion of earthquake and rain induced rapid landslides and its application to the 2006 Leyte landslide, Landslides, Vol. 7, No. 3, pp. 219-236.

Sassa, K., He, B., Miyagi, T., Strasser, M., Konagai, K., Ostric, M., Setiawan, H., Takara, K., Nagai, O., Yamashiki, Y. and Tutumi, S. (2012): A hypothesis of the Senoumi submarine megaslide in Suruga Bay in Japan—based on the undrained dynamic-loading ring shear tests and computer simulation, Landslides, Vol. 9, No. 4, pp. 439–455.

Sassa, K., Dang, K., He, B., Takara, K., Inoue, K. and Nagai, O. (2014a): A new high-stress undrained ring-shear apparatus and its application to the 1792 Unzen-Mayuyama megaslide in Japan, Landslides, Vol. 11, No. 5, pp. 827-842.

Sassa, K., Fukuoka, H., Sato, Y., Takara, K., Huy, L., Setiawan, H., Pham, T. and Dang, K. (2014b): Initiation mechanism of rapid and long runout landslides and simulation of Hiroshima landslide disasters using the integrated simulation model (LS-RAPID). Proc. of the International Forum “Urbanization and Landslide Disaster, 85-112 (in Japanese).

Senthilkumar, V., Chandrasekaran, S.S. and Maji, V.B. (2017): Geotechnical characterization and analysis of rainfall—induced 2009 landslide at Marappalam area of Nilgiris district, Tamil Nadu state, India, Landslides, Vol. 14, No. 5, pp. 1803-1814.

Setiawan, H., Sassa, K., Takara, K., Miyagi, T. and Fukuoka, H. (2016): Initial pore Pressure Ratio in the Earthquake Triggered Large-scale Landslide near Arotazawa Dam in Miyagi Prefecture, Japan, Procedia Earth and Planetary Science, Vol. 16, pp. 61-70.

Setiawan, H., Sassa, K., Takara, K., Miyagi, T. and Fukuoka, H. (2017): Detail Study of the Aratozawa Large-Scale Landslide in Miyagi Prefecture, Japan. In: Mikoš, M., Vilimek, V., Yin, Y., Sassa, K. (eds.): Advancing Culture of Living with Landslides. Vol. 5 - Landslides in Different Environments: 473-480.

Sodnik, J., Kumelj, Š., Peternel. T., Jež, J. and Maček, M. (2017): Identification of Landslides as Debris Flow Sources Using a Multi-model Approach Based on a Field Survey - Koroška Bela, Slovenia, In: Mikoš, M., Tiwari, B., Yin, Y., Sassa, K. (eds.): Advancing Culture of Living with Landslides, Vol. 2 - Advances in Landslide Science, pp. 1119-1126.

Tien, P.V., Sassa, K., Takara, K., Dang, K., Luong, L.H. and Ha, N.D. (2017): Simulating the Formation Process of the Akatani Landslide Dam Induced by Rainfall in Kii Peninsula, Japan, In: Mikoš, M., Vilimek, V., Yin, Y., Sassa, K. (eds.): Advancing Culture of Living with Landslides. Vol. 5 - Landslides in Different Environments, pp. 497-506.

Tsuchiya, S., Kyoji, S. and Nagai, O. (2013): Simulation of the Largest Landslide Caused by the 2008 Wenchuan Earthquake by Rapid-Landslide-Movement Simulation, In: Ugai, K., Yagi, H., and Wakai, A. (eds.): Earthquake-Induced Landslides, Springer Verlag, Berlin, Heidelberg, pp. 575-582.

Vidoda Prodan, M. and Arbanas, Ž. (2017): Parametric Analysis of Weathering Effect on Possible Reactivation of the Valići Landslide, Croatia, In: Mikoš, M., Tiwari, B., Yin, Y., Sassa, K. (eds.): Advancing Culture of Living with Landslides, Vol. 2 - Advances in Landslide Science, pp. 621-631.

Yavari-Ramshe, S. and Ataie-Ashtiani, B. (2016): Numerical modeling of subaerial and submarine landslide-generated tsunami waves - recent advances and future challenges, Landslides, Vol. 13, No. 6, pp. 1325-1368.